Hermite Interpolation by Pythagorean Hodograph Curves in Euclidean and Minkowski Space

J. Kosinka, Z. Šír and B. Jüttler
Institute of Applied Geometry, JKU Linz

Abstract: A survey of some new results about Hermite interpolation by Pythagorean Hodograph curves is given. In particular we discuss the C^2 interpolation in Euclidean plane and space and the G^1 interpolation in Minkowski space. We give an outline of our methods and results together with examples and references to relevant papers. *Keywords*: Hermite interpolation, Pythagorean hodograph curves, Minkowski space

1 Introduction

Pythagorean hodograph (PH) curves (see the survey [4] and the references cited therein), form a remarkable subclass of polynomial parametric curves. They have a piecewise polynomial arc length function and, in the planar case, rational offset curves. These curves provide an elegant solution of various difficult problems occurring in applications, in particular in the context of CNC (computer-numerical-control) machining.

Curves in Minkowski space $\mathbb{R}^{2,1}$ are very well suited to describe the medial axis transform (MAT), which plays a key role in the definition of Minkowski Pythagorean hodograph (MPH) curves. A curve in $\mathbb{R}^{2,1}$ considered as a MAT uniquely defines a planar domain. Minkowski Pythagorean hodograph curves correspond to domains, where both the boundaries and their offsets are rational curves, [15].

Our paper is devoted to the Hermite interpolation by (M)PH curves, which seems to the most promising among various methods for their construction. Since it is essentially a local construction, it results in a relatively reasonable system of nonlinear equations, which can be explicitly solved in certain cases. Other (global) methods lead typically to a huge system of nonlinear equation having unclear solvability condition. As an additional problem it is necessary to make a choice among a great number of solutions.

The remainder of the paper is organized as follows. After recalling some basic facts about PH curves in Euclidean and Minkowski space we outline our results about C^2 Hermite interpolation in Euclidean space in the context of other interpolation techniques. Afterwards, we give a survey of G^1 Hermite interpolation by MPH cubics focusing on solvability and approximation order. We also present a brief outline of converting analytic curves into MPH cubic splines. Finally we conclude the paper.

2 Euclidean and Minkowski PH curves

In this section we summarize some basic properties of Pythagorean Hodograph curves in both Euclidean and Minkowski spaces.

A Bézier curve is called *Pythagorean Hodograph (PH)* if the length of its tangent vector, taken in the appropriate metric, depends in a polynomial way on the parameter. In particular

- $\mathbf{p}(t) = [x(t), y(t)]$ is called *planar PH curve* if there exists a polynomial $\sigma(t)$ such that

$$x'(t)^2 + y'(t)^2 = \sigma^2(t), \tag{1}$$

- $\mathbf{p}(t) = [x(t), y(t), z(t)]$ is called a *spatial PH curve* if there exists a polynomial $\sigma(t)$ such that

$$x'(t)^2 + y'(t)^2 + z'(t)^2 = \sigma^2(t), \quad \text{and} \tag{2}$$

- $\mathbf{p}(t) = [x(t), y(t), z(t)]$ is called a *spatial Minkowski PH (MPH) curve* if there exists a polynomial $\sigma(t)$ such that

$$x'(t)^2 + y'(t)^2 - z'(t)^2 = \sigma^2(t). \tag{3}$$

The degree of $\sigma(t)$ equals $n - 1$, where n is the degree of the PH curve. The curve $\mathbf{h}(t) = [x'(t), y'(t)\{, z'(t)\}]$ is called the *hodograph* of $\mathbf{p}(t)$.

The planar polynomial curve $\mathbf{p}(t)$ can be identified with complex valued polynomial $\mathbf{p}(t) = x(t) + iy(t)$. The hodograph $\mathbf{h}(t) = x'(t) + iy'(t)$ then satisfy the equation (1) if and only if it is of the form $\mathbf{h}(t) = \mathbf{w}(t)^2$, where $\mathbf{w}(t) = v(t) + iw(t)$ is a complex valued polynomial called *preimage*, [3].

In a similar way, the spatial polynomial curve $\mathbf{p}(t)$ can be identified with pure–quaternion–valued polynomial $\mathbf{p}(t) = x(t)\mathbf{i} + y(t)\mathbf{j} + z(t)\mathbf{k}$. The hodograph $\mathbf{h}(t) = x'(t)\mathbf{i} + y'(t)\mathbf{j} + z'(t)\mathbf{k}$ then satisfy the equation (2) if and only if it is of the form $\mathbf{h}(t) = \mathcal{A}(t)\,\mathbf{i}\,\mathcal{A}^*(t)$, where $\mathcal{A}(t) = u(t) + v(t)\mathbf{i} + p(t)\mathbf{j} + q(t)\mathbf{k}$ is a quaternion valued polynomial called *preimage*, [2].

In the Hermite interpolation one wants to construct a suitable object (a PH curve in our case) matching prescribed boundary data. This data are typically the end point positions and some additional constraints, which can be analytical (derivative vectors) or geometrical (tangent directions, curvature, etc.) information. In the former case we talk about C-interpolation, in the latter about G-interpolation.

As an immediate consequence of the definition of MPH curves, the tangent vector $\mathbf{c}'(t)$ of an MPH curve cannot be time–like. Also, light–like tangent vectors $\mathbf{c}'(t)$ correspond to roots of the polynomial $\sigma(t)$ in (3). In the remainder of this paper we consider only curves with space–like tangent vectors. These curves will be called space–like. Recall that the MAT of a planar domain is a space curve with space–like or light–like tangent vectors, where the latter ones appear only at isolated points, typically at vertices (points with extremal curvature) of the boundaries.

data	degree	maximum number of solutions and computational effort	available results
		2D-plane	
G^1	3	2 solutions, quadratic equation (Walton and Meek [14])	One of the solutions has approximation order 4 at generic points [14].
C^1	5	4 solutions, quadratic equations (Farouki and Neff [7])	The best solution can be identified via its rotation index (Moon et al. [16]).
$G^2[C^1]$	7	8 solutions, quartic equations (Jüttler [10])	One of the solutions has approximation order 6 at generic points [10]. Inflections reduce the approximation order.
C^2	9	4 solutions, quadratic equations (Farouki et al. [6])	One of the solutions has approximation order 6 at all points (Šír and Jüttler [17]).
		3D-space	
G^1	3	2 solutions, quadratic equation (Jüttler and Mäurer [11])	One of the solutions has approximation order 4 at generic points (Mäurer and Jüttler [13]).
C^1	5	2–parametric system of solutions, quadratic equations in quaternions (Farouki and Neff [5])	One solution has the best approximation order 4, preserves planarity and symmetry of the data (Šír and Jüttler [19]).
C^2	9	4–parametric system of solutions, quadratic and linear equations in quaternions (Šír and Jüttler [18])	One solution has the best approximation order 6, preserves planarity and symmetry of the data [18].

Table 1: Hermite interpolation by Euclidean PH curves.

3 C^2 Hermite interpolation in Euclidean plane and space

Table 1 summarizes the known results about Hermite interpolation in the Euclidean plane and space. One can observe two facts. First, interpolation of geometrical data is in principle more complicated then that of analytical data. Only the G^1 construction is available both in space and plane. The combined $G^2[C^1]$ interpolation in plane leads to the most complicated (quartic) equations. Moreover, while the C-interpolation has always a solution, this is not the case for G-interpolation, where certain conditions of solvability exist. Second, the space yields more freedom to satisfy the PH condition and therefore there are more interpolants of the same degree than in the plane.

Recently we gave new results concerning C^2 Hermite interpolation [17] and [18]. The task is to construct a PH curve $\mathbf{p}(t)$ matching given C^2 Hermite boundary data: the end points $\mathbf{p}_b$, $\mathbf{p}_e$, the first derivative vectors (velocities) $\mathbf{v}_b$, $\mathbf{v}_e$ and the second derivative vectors (accelerations) $\mathbf{a}_b$, $\mathbf{a}_e$. This can be done most efficiently by constructing the preimage. If we work in a suitable polynomial basis (such as Bernstein Bézier basis), the boundary condition which are linear for the curve $\mathbf{p}(t)$ and its hodograph $\mathbf{h}(t)$ become non-linear for the preimage $\mathbf{w}(t)$ or $\mathcal{A}(t)$.

	2D-plane, complex numbers		3D-space, quaternions	
	Equation	#Solutions	Equation	#Solutions
quadratic	$\mathbf{x}^2 = \mathbf{a}$	2	$\mathcal{X}\mathbf{i}\mathcal{X}^* = \mathcal{A}$	1-param. system
linear	$\mathbf{x}\mathbf{b} = \mathbf{a}$	1	$\mathcal{X}\mathcal{B} = \mathcal{A}$	1-param. system

Table 2: Two types of equation occurring in the C^2 Hermite interpolation process. The unknowns are $\mathbf{x}$ (complex number) or $\mathcal{X}$ (quaternion).

The resulting system can be however reduced to successive explicit solution (in quaternions or complex numbers) of several equations which are quadratic or linear (see Table 2).

While the complex number equation have a finite number of solution, the quaternion ones have one dimensional systems of solutions. We thus obtain a finite number of preimages for the planar case and multidimensional system of preimages in the space case. After eliminating some redundancies we finally obtain four PH interpolants in the planar case and a four dimensional system of solutions in the space case. Via an asymptotical analysis we were able to identify the ”best” solution, which behaves in a most suitable way, when we interpolate data taken from an analytical curve and we diminish the step size.

As an example, Figure 1, left shows the system of spatial PH interpolants of degree 9 to the data

$$\begin{array}{lllllllll} \mathbf{p}_b & = & [0,0,0], & \mathbf{v}_b & = & [3,0,0], & \mathbf{a}_b & = & [0,1,0] \\ \mathbf{p}_e & = & [1,1,0], & \mathbf{v}_e & = & [3,0,0], & \mathbf{a}_e & = & [0,-1,0]. \end{array} \tag{4}$$

Note that these data lie in fact in the xy-plane and therefore the four dimensional system of spatial interpolants must contain the four planar interpolants (shown on the right figure).

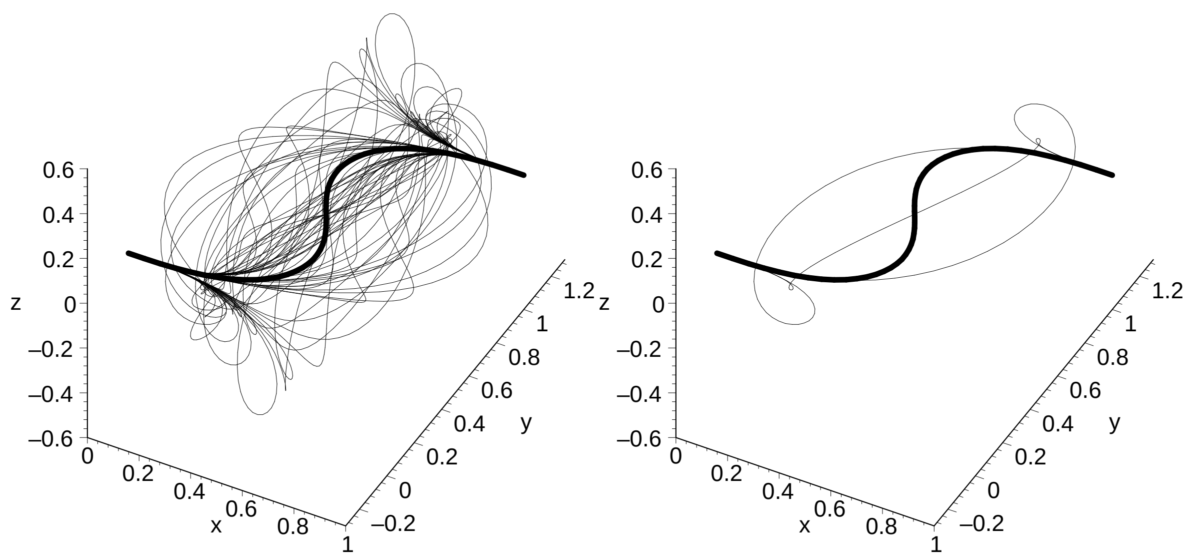

Figure 1: Left figure shows 64 representants of the four dimensional system of PH interpolants of the data (4). Right figure shows 4 interpolants, which are planar. The ”best” interpolant is plotted in bold.

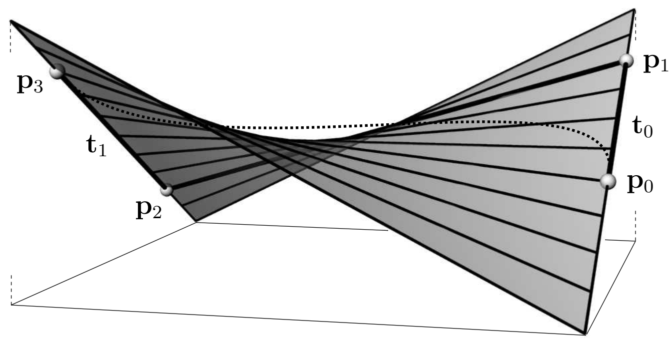

Figure 2: Necessary condition: the control polygon of the interpolating MPH cubic lies on a certain hyperbolic paraboloid.

4 Hermite interpolation in Minkowski space

In this section we summarize some results concerning G^1 Hermite interpolation by cubic MPH curves and an approximate conversion of a space–like analytic curve into MPH cubic spline.

4.1 G^1 Hermite interpolation by MPH cubics

Let us consider an MPH cubic $\mathbf{g}(t)$ in Bézier form

$$\mathbf{g}(t) = \mathbf{p}_0\,(1-t)^3 + \mathbf{p}_1\,3t(1-t)^2 + \mathbf{p}_2\,3t^2(1-t) + \mathbf{p}_3\,t^3,\ t \in [0,1], \tag{5}$$

which is to interpolate two given points $\mathbf{q_0} = \mathbf{p}_0$ and $\mathbf{q_1} = \mathbf{p}_3$, and the associated space-like unit tangent directions $\mathbf{t}_0$ and $\mathbf{t}_1$. It turns out that this interpolation problem leads to two quadratic equations, which yield up to four distinct MPH cubic interpolants. A necessary condition for the interpolants is that their control polygons lie on a certain hyperbolic paraboloid, see Fig. 2.

In order to analyze the solvability of the problem, we shall simplify the given input data without loss of generality as far as possible. First, we move the starting point $\mathbf{p}_0$ of the curve $\mathbf{g}(t)$ to the origin, while the endpoint $\mathbf{p}_3$ remains arbitrary. Then we apply Lorentz transforms to map the input data to one out of five canonical positions depending on the causal characters of the sum and difference of $\mathbf{t}_0$ and $\mathbf{t}_1$. In order to obtain solutions, the endpoint $\mathbf{q}_1$ has to lie inside certain quadratic cone, which depends solely on the input Hermite data, see Fig. 3. A thorough discussion of the number of interpolants is given in [12].

4.2 Converting analytic curves into MPH cubic splines

Let us consider a space–like curve segment $\mathbf{p} = \mathbf{p}(s)$ with $s \in [0, S_{max}]$ in Minkowski space. The coordinate function are assumed to be analytic. For a given step–size h, we generate points and tangents at the points $s = ih$, $i = 0, 1, 2, \ldots$, and apply the G^1 Hermite interpolation

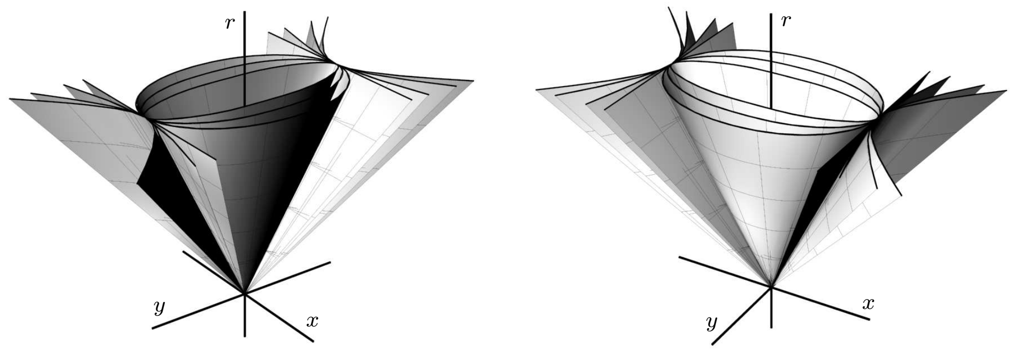

a) b)

Figure 3: Space–like difference vector and two corresponding families of quadratic cones.

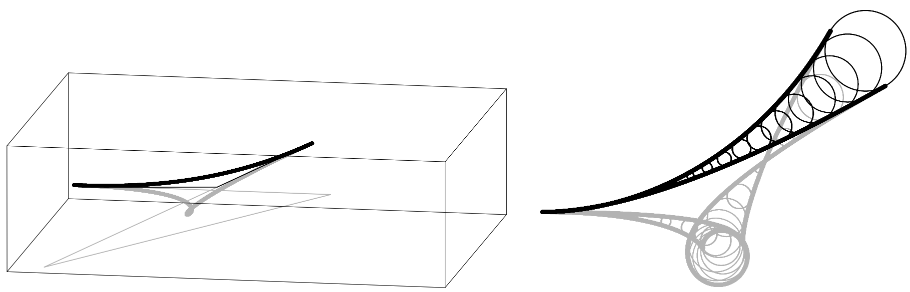

a) b)

Figure 4: a) Two interpolants to given medial axis transform, b) corresponding circles and their rational envelopes.

procedure by MPH cubics to the pairs of adjacent points and tangents. With the help of Taylor expansions we analyze the existence and the behavior of the solutions for decreasing step–size $h \to 0$.

If the principal normal vector of $\mathbf{p}$ is space–like or time–like, the G^1 interpolation has four solutions, provided that the step–size $h > 0$ is sufficiently small. Exactly one among them matches the orientation of the given tangent vectors. This solution has the approximation order four. The approximation order reduces to two at isolated Minkowski inflections, i.e. when the principal normal vector of $\mathbf{p}$ is light–like for $s = 0$.

4.3 Example

Consider the space–like cubic arc (the MAT of a planar domain Ω) $\mathbf{h}(t) = (t, t^2, \frac{t^3}{2})^\top$, $t \in [0, \frac{1}{2}]$. We apply the G^1 Hermite interpolation scheme to this curve segment. Two among the four interpolants are shown in Fig. 4 along with the rational approximations to the original domain boundary $\partial\Omega$.

5 Conclusion

The described constructions represent the state of art of the Hermite interpolation by PH curves. We were able to obtain construction methods along with an analysis of the quality of the solutions. In this way we described the solution which can be used for example for conversion of analytical curves into PH splines or (in the Euclidean case) for smoothing tool paths.

Based on the mutual position of the given first order Hermite data we described the basic results concerning the conditions for the existence and the number of MPH cubic interpolants. Moreover, we presented an approach to the approximate conversion of a space–like analytic curve into MPH cubic spline. The approximation order is generally equal to four, but it reduces to two at isolated Minkowski inflections.

Acknowledgment.

The first two authors were supported through grant P17387-N12 of the Austrian Science Fund (FWF).

References

[1] H. I. Choi, Ch. Y. Han, H.P. Moon, K. H. Roh & N.S. Wee (1999), Medial axis transform and offset curves by Minkowski Pythagorean hodograph curves, Computer–Aided Design, 31, 59–72.

[2] H.I. Choi, D.S. Lee & H.P. Moon (2002), Clifford algebra, spin representation, and rational parameterization of curves and surfaces. Adv. Comput. Math. 17, 5–48.

[3] R.T. Farouki (1994), The conformal map $z \to z^2$ of the hodograph plane. Comp. Aided Geom. Design 11, 363–390.

[4] R.T. Farouki (2002), Pythagorean–hodograph curves, Handbook of Computer Aided Geometric Design (J. Hoschek, G. Farin & M.-S. Kim, eds.), Elsevier, 405–427.

[5] R.T. Farouki, M. al-Kandari & T. Sakkalis (2002), Hermite interpolation by rotation-invariant spatial Pythagorean-hodograph curves., Adv. Comput. Math. 17, 369–383.

[6] R.T. Farouki, J. Manjunathaiah & S. Jee (1998), Design of rational cam profiles with Pythagorean-hodograph curves. Mech. Mach. Theory 33, 669–682.

[7] R.T. Farouki & C.A. Neff (1995), Hermite interpolation by Pythagorean-hodograph quintics, Math. Comput. 64, 1589–1609.

[8] R.T. Farouki & Sakkalis T. (1990), Pythagorean hodographs, IBM Journal of Research and Development, 34, 736–752.

[9] R.T. Farouki & T. Sakkalis (1994), Pythagorean-hodograph space curves, Adv. Comput. Math. 2, 41–66.

[10] B. Jüttler (2001), Hermite interpolation by Pythagorean hodograph curves of degree seven. Math. Comp. 70, 1089–1111.

[11] B. Jüttler & C. Mäurer (1999), Cubic Pythagorean Hodograph Spline Curves and Applications to Sweep Surface Modeling, Comp.–Aided Design 31, 73–83.

[12] J. Kosinka, & B. Jüttler, G^1 Hermite Interpolation by Minkowski Pythagorean Hodograph Cubics, submitted to CAGD.

[13] C. Mäurer & B. Jüttler (1999), Rational approximation of rotation minimizing frames using Pythagorean–hodograph cubics, Journal for Geometry and Graphics 3, 141–159.

[14] D.S. Meek & D.J. Walton (1997), Geometric Hermite interpolation with Tschirnhausen cubics, Journal of Computational and Applied Mathematics 81, 299–309.

[15] H.P. Moon (1999), Minkowski Pythagorean hodographs, Computer Aided Geometric Design, 16, 739–753.

[16] H.P. Moon, R.T. Farouki & H.I. Choi (2001), Construction and shape analysis of PH quintic Hermite interpolants, Comp. Aided Geom. Design 18, 93–115.

[17] Z. Šír & B. Jüttler (2004), Constructing acceleration continuous tool paths using pythagorean hodograph curves. Mech. Mach. Theory. To appear. Preprint available at www.ag.jku.at/jue_pub_en.html.

[18] Z. Šír & B. Jüttler (2005), C^2 Hermite interpolation by space Pythagorean Hodograph curves, submitted to Adv. Comput. Math.

[19] Z. Šír & B. Jüttler (2005), Spatial Pythagorean Hodograph Quintics and the Approximation of Pipe Surfaces, to appear at Mathematics of Surfaces 2005. Preprint available at www.ag.jku.at/jue_pub_en.html.

[20] J. Walrave (1995), Curves and surfaces in Minkowski space, Doctoral thesis, K. U. Leuven, Fac. of Science, Leuven.

Jiří Kosinka, Zbyněk Šír and Bert Jüttler
Institute of Applied Geometry
Johannes Kepler University
Altenberger Str. 69
A–4040 Linz, Austria